

This work was written as part of one of the author's official duties as an Employee of the United States Government and is therefore a work of the United States Government. In accordance with 17 U.S.C. 105, no copyright protection is available for such works under U.S. Law.

Public Domain Mark 1.0

<https://creativecommons.org/publicdomain/mark/1.0/>

Access to this work was provided by the University of Maryland, Baltimore County (UMBC) ScholarWorks@UMBC digital repository on the Maryland Shared Open Access (MD-SOAR) platform.

**Please provide feedback**

Please support the ScholarWorks@UMBC repository by emailing [scholarworks-group@umbc.edu](mailto:scholarworks-group@umbc.edu) and telling us what having access to this work means to you and why it's important to you. Thank you.

# PROCEEDINGS OF SPIE

[SPIDigitalLibrary.org/conference-proceedings-of-spie](https://spiedigitallibrary.org/conference-proceedings-of-spie)

## Optical and fluorescence properties of corn leaves from different nitrogen regimes

Elizabeth Middleton, James McMurtrey, Petya Entcheva Campbell, Lawrence Corp, L. Butcher, et al.

Elizabeth M. Middleton, James E. McMurtrey III, Petya K. Entcheva Campbell, Lawrence A. Corp, L. Maryn Butcher, Emmett W. Chappelle, "Optical and fluorescence properties of corn leaves from different nitrogen regimes," Proc. SPIE 4879, Remote Sensing for Agriculture, Ecosystems, and Hydrology IV, (17 March 2003); doi: 10.1117/12.463087

**SPIE.**

Event: International Symposium on Remote Sensing, 2002, Crete, Greece

# \*Optical and fluorescence properties of corn leaves from different nitrogen regimes

Elizabeth Middleton<sup>a\*</sup>, James E. McMurtrey<sup>b</sup>, Petya K. Entcheva Campbell<sup>a</sup>, Larry A. Corp<sup>a,b</sup>,  
L. Maryn Butcher<sup>a,b</sup>, and Emmett W. Chappelle<sup>a,b</sup>

<sup>a</sup> National Aeronautics and Space Agency/Goddard Space Flight Center, Greenbelt, MD 20771 USA

<sup>b</sup> Agricultural Research Service, US Department of Agriculture, Beltsville, MD 20705 USA

## ABSTRACT

The important role of nitrogen (N) in limiting or enhancing vegetation productivity is relatively well understood, although the interaction of N with other environmental variables in natural and agricultural ecosystems needs more study. In 2001, a suite of optical, fluorescence, and biophysical measurements were collected on leaves of corn (*Zea Mays* L.) from field plots provided four N fertilizer application rates: 20%, 50%, 100% and 150% of optimal N levels. Two complementary sets of high-resolution (< 2 nm) optical spectra were acquired for both adaxial and abaxial leaf surfaces. The first was comprised of leaf optical properties (350-2500 nm) for reflectance, transmittance, and absorbance. The second was comprised of reflectance spectra (500-1000 nm) acquired *with* and *without* a long pass 665 nm filter to determine the fluorescence contribution to “apparent reflectance” in the 670-750 nm spectrum that includes the 685 and 740 nm chlorophyll fluorescence (ChlF) peaks. Two types of fluorescence measurements were also made on adaxial and abaxial surfaces: 1) fluorescence images in four 10 nm bands (blue, green, red, far-red) resulting from broadband irradiance excitation; and 2) emission spectra at 5 nm resolution produced by three excitation wavelengths (280, 380, and 532 nm). The strongest relationships between optical properties and foliar chemistry were obtained for a “red-edge” optical parameter versus C/N and chlorophyll *b*. Select optical indices and ChlF parameters were correlated. A significant contribution of steady-state ChlF to apparent reflectance was observed, averaging 10-25% at 685 nm and 2-6% at 740 nm over the range of N treatments. From all measurements assessing fluorescence, higher ChlF was measured from the abaxial leaf surfaces.

**Keywords:** high spectral resolution reflectance and fluorescence, chlorophyll fluorescence, carbon/nitrogen ratio, chlorophyll *b*, red edge, nitrogen deficiency and excess.

## 1. INTRODUCTION

Carbon cycle science is a primary focus in current Earth science studies, for which the identification or development of appropriate remote sensing techniques to quantify carbon sinks or sources is essential. A primary driving force behind carbon uptake and storage by vegetation is the availability of soil nitrogen (N). In terrestrial ecology and agricultural studies, the physiological status of vegetation has typically been inferred from spectral indices derived from relatively broadband satellite or aircraft sensors. The most common optical spectral indices (e.g., the Normalized Difference Vegetation Index, NDVI) combine the reflectances (R) in the red (Red) and far-red (FR) spectral regions to express the relative change in amplitude from a red minimum to a near-infrared maximum, across a region referred to as the “red edge”. The NDVI and other optical spectral indices have been used to estimate a suite of variables associated with the greenness of vegetation, including chlorophyll content and leaf area index. Current satellite based optical remote sensing techniques employ relatively wide ( $\geq 20$  nm) spectral bands to monitor vegetation status and change over time. Laboratory, field, aircraft (e.g., AVIRIS), and satellite (e.g., EO-1 Hyperion) studies have all demonstrated that additional spectral information can be retrieved in the red edge region from derivative analysis of high resolution (<10 nm) spectra [1, 2, 3, 4, 5]. The additional spectral information enables estimation of the change in slope at the red edge, expressed as the first derivative maximum (Dmax), and the red edge is defined as the wavelength at which Dmax occurs. These red-edge parameters are influenced by chlorophyll content [2, 4, 5]. At the same time, the importance of the Red and FR spectral regions for the assessment of photosynthetic function using chlorophyll fluorescence (ChlF), which produces peaks at 685 and 740 nm, has been well established in laboratory studies [6]. Fluorescence peaks in the blue and green spectra, or ratios to ChlF peaks (e.g., Red/FR and Red/blue fluorescence emission ratios), have also been

---

\*[betsym@ltpmail.gsfc.nasa.gov](mailto:betsym@ltpmail.gsfc.nasa.gov); phone, +01 301-614-6670; fax, +01 301-614-6695; Biospheric Sciences Branch, Laboratory for Terrestrial Physics, Code 923, NASA/GSFC, Greenbelt, MD 20771, USA

related to vegetation vigor [7, 8, 9, 10, 11, 12]. However, the links among ChlF, blue/green emissions, and the red edge optical spectra have not been well studied, nor has the role of nitrogen (N) in influencing the spectral properties of foliage in the red edge.

Our goal was to evaluate the relative usefulness of high spectral resolution (<10 nm) optical and fluorescence measurements to distinguish leaf-level physiologic status and to determine whether any spectral index was capable of discerning parameters of interest to carbon allocation, N utilization, and/or photosynthetic function in leaves. Plant material was obtained from an agricultural field study where corn (*Zea mays* L.) was grown under different N fertilizer application regimes. Measurements were focused during four weeks of a seven-week period in August and September, near the end of the growing season when foliar chemistry was changing as nutrients were translocated from leaves to reproductive organs, including the developing ear. Our primary objective was to acquire an integrated data set comprised of biological, optical and fluorescence data, for comparative analyses.

## 2. METHODOLOGY

### 2.1 Plant Material

Leaves were obtained from corn (*Zea mays* L.), a C<sub>4</sub> species, grown under a gradient of inorganic N fertilization levels in 2001 at the USDA Agricultural Research Center in Beltsville MD, USA as part of a larger project for “Optimizing Production Inputs for Economic and Environmental Enhancement (OPE<sup>3</sup>)”, designated as a NASA MODIS Validation Site. The four N fertilizer application rates on field plots (210, 140, 70, and 28 kg N/ha) provided 150%, 100%, 50% and 20% of the optimal recommended N level for corn on soils in central Maryland, ranging from excess to deficient soil N levels. Leaf-level measurements were obtained on the third from terminal leaf on four days during early August when corn was in the vegetative stage, and on five days in September over a two week period at the grain fill (R3) reproductive stage near the end of the growing season.

### 2.2 Leaf Biophysical Measurements

The following biophysical data were collected on each fresh leaf sample: 1) photosynthetic pigment concentration ( $\mu\text{g cm}^{-2}$ ) for chlorophyll *a* (Chl *a*), chlorophyll *b* (Chl *b*), and total carotenoids; 2) leaf area ( $\text{cm}^2$ ) determined with a Leaf Area Meter (Li-Cor, Inc. Lincoln NE, USA); and 3) photosynthetic capacity, Amax ( $\mu\text{mol CO}_2 \text{ m}^{-2} \text{ s}^{-1}$ ) determined with a Li-Cor 6400 Photosynthetic System. Amax was determined under controlled conditions of high photosynthetically active radiation (PAR) illumination intensity ( $1800 \mu\text{mol PAR m}^{-2} \text{ s}^{-1}$ ), saturating CO<sub>2</sub> concentration (1000 ppm), leaf chamber temperature (25° C), and relative humidity (~35%). Pigment concentrations were determined on leaf discs extracted in 3.5 ml dimethyl sulfoxide (DMSO) using standard equations [13] and absorption coefficients at 4 wavelengths (470, 640, 648, and 750 nm) obtained with a dual-beam Lambda 4 spectrophotometer (Perkin-Elmer, Norwalk CN, USA). Specific leaf mass ( $\text{g/m}^2$ ) was determined on dried leaf samples (AE260, Mettler Toledo, Columbus OH, USA). Elemental C-H-N composition was determined from dried and ground leaf material (CHN-600 Elemental Analyzer System 785-500, LECO Corp., St. Joseph MO, USA) at the University of Maryland (College Park MD, USA) using the Dumas combustion method for determination of C, N and H levels by percent dry mass.

### 2.3 Fluorescence Emission Spectra

A spectrofluorometer (Fluorolog II, Spex Industries, Edison NJ, USA) having two 0.22 m double monochrometers was used to produce and collect fluorescence emission spectra. The excitation monochromator (2 mm slit width = 3.4 nm resolution) was attached to a 450 W xenon lamp, which allowed variation of the excitation radiation. The emission monochromator (2 mm slit width = 3.4 nm resolution) was attached to a photon-counting photomultiplier tube corrected to obtain linearity throughout the emission wavelength range of 290 to 850 nm while voltage readings were calibrated to photon counts per second (cps). Fluctuations in lamp intensity were corrected by using a beam splitter to deliver a portion of the excitation radiation to a rhodamine dye cuvette to monitor fluorescence response by a silicon photo diode. This response was used to generate correction factors for equalizing changes in lamp intensity as a function of wavelength [14]. Leaf samples were placed in a solid, non-fluorescent anodized aluminum sample holder. Spectra were collected at a resolution of 5 nm, with leaf samples displaying first adaxial (top) and then abaxial (bottom) surfaces. To prevent light-induced changes in the region viewed, the illuminated leaf area was shifted to a slightly different sector of the central leaf surface when the leaf was turned from the adaxial to abaxial surface. Three excitation wavelengths were used: 280 nm (280EX), 380 nm (380EX), and 532 nm (532EX) [added in September only], with emission spectra recorded between 300-800 nm, 400-800 nm, and 600-800 nm respectively. Consequently, either four (August) or six

(September) spectra were obtained per sample (3 excitation wavelengths for adaxial and abaxial surfaces), recorded in counts per second (cps). From the 280EX spectra, emissions were selected as primary responses at 320, 440, 525, 685, and 740 nm, and fluorescence ratios were calculated (e.g., 320F/440F, 440F/525F, 685F/740F). From the 380EX spectra, emissions at 455, 530, 685, and 740 nm were selected as primary, and fluorescence ratios were calculated (e.g., 455F/530F; 685F/455F; 685F/530F; 685F/740F; 740F/530F). Emissions at the 685 and 740 nm ChlF peaks were also extracted from the 532EX spectra. The 685F/740F ratios calculated from 380EX and 532EX peaks were designated as Red/FR<sub>EX380</sub> and Red/FR<sub>EX532</sub>, respectively.

## 2.4 Fluorescence Emission Images

A dark room fluorescence imaging system (FIS) was used to quantify leaf fluorescence emissions in four discrete 10 nm bands in the blue, green, red, and far-red regions [15]. The imaging system consists of a UV excitation source having nearly uniform illumination intensity of 0.33 mW cm<sup>-2</sup> centered at 365 nm; an intensified thermoelectrically-cooled charge-coupled device (CCD) camera capable of capturing 16 bit, 1036 X 1032 pixel image; and a computer interface for data collection, filter wheel and camera control. The automated filter wheel (AB300, CVI Laser Corp., Albuquerque NM, USA) contains four interference filters with 10 nm FWHM (full width at half maximum) centered at 450 nm (blue band), 550 nm (green band), 680 nm (red band), and 740 nm (far-red band). The camera responsivity and variation due to non-uniform illumination for the system were calibrated using a flat field fluorescent target. Dark current responses of the camera were subtracted for each image and thermal corrections for the cooled CCD camera were applied. Leaf samples were placed on a black, non-fluorescent tray below the CCD. Integration times were adjusted per band each day to ensure adequate dynamic ranges for measurements and intensities are reported in digital counts per second (dcps). Eight images per sample were acquired, 4 bands each per adaxial and abaxial leaf surface. FIS images were processed using special software packages (ENVI and IDL, Research Systems Incorporated, Boulder CO, USA). Images for the four spectral bands were co-registered to enable calculation of band ratios, and threshold values were used to constrain the region of interest before descriptive statistics were calculated.

## 2.5 Leaf Optical Property Measurements

Spectral leaf optical properties were determined on both adaxial (top, T) and abaxial (bottom, B) leaf surfaces. Spectral measurements were acquired by using an integrating sphere (Li-Cor 1800) attached to an ASD spectroradiometer (ASD-FR FieldSpec®Pro, Analytical Spectral Devices, Inc., Boulder CO, USA) having a 1.4 nm sampling interval and an effective spectral resolution of < 2 nm (3 nm FWHM) in the 350 - 2500 nm range. Reflectance (R), transmittance (Tr), and absorptance (A) spectra were produced for both leaf surfaces. Optical spectra are described herein for adaxial and abaxial reflectance (RT and RB); adaxial transmittance (TrT≈TrB); and absorptance determined from the adaxial surface (AT). Twenty published spectral indices were calculated from each spectrum [5, 16, 17, 18, 19, 20]. On each original leaf spectrum for RT, RB, TrT, and AT, a first derivative spectrum was computed and several red edge derivative parameters were determined. The red edge derivative parameters included the maximum derivative (Dmax) occurring between 690 and 730 nm, the wavelength at which Dmax occurred, and derivatives at 704, 714, and 744 nm (D704, D714, D744). Several derivative indices were calculated, including Dmax/D744.

## 2.6 Contributions of Chlorophyll Fluorescence to Apparent Reflectance

Optical data were collected on an adjacent section of each leaf to measure the spectra in the ChlF region *with* and *without* induction of chlorophyll fluorescence. Spectral measurements were conducted using procedures established by Kim [21] and further developed by Zarco-Tejada [19] and by Entcheva-Campbell [22]. These high spectral resolution measurements (~2 nm) were acquired using a second ASD spectroradiometer (FR FieldSpec®Pro) with the same characteristics as described above and an 8° sensor foreoptic viewing a leaf area of approximately 2 cm<sup>2</sup>. A 300W xenon arc lamp coupled with a set of neutral density filters was used to simulate constant solar radiation (10am, June, Beltsville MD). A halogen panel was used as a reference standard. Samples were placed upright in leaf holders.

Most ChlF can be prevented by blocking absorption of light in wavelengths < 665 nm because fluorescence emissions result from photons absorbed at shorter (~ 20 nm) wavelengths, and the two ChlF peaks are centered at longer (≥20 nm) wavelengths-- 685 and 740 nm. A Schott RG 665 long pass filter was placed in front of the light source to prevent ChlF induction, allowing the determination of reflectance (R) alone. Without the filter, however, the unfiltered irradiation induced ChlF, and the quantity measured was “apparent reflectance” ( $R_a = R + F$ )<sub>λ</sub>. Samples were dark adapted for 5 minutes immediately before initiating the  $R_a$  measurements.  $R$  and  $R_a$  spectra across the 650 - 800 nm region were recorded every 0.01 s for 25 seconds. The ChlF contribution to  $R_a$  per wavelength was calculated as the difference,

$(R_a - R)_\lambda$ . Estimates of the maximum ChlF ( $F_{max}$ ) and the steady state ChlF ( $F_s$ ) were expressed as a percentage of the incoming radiation. The differences in ChlF recovery trends, during decay from  $F_{max}$  to  $F_s$ , were assessed with  $F_{slope}$ . This is the first derivative maximum of the F685 and F740 nm responses over the time of consecutive scanning.

## 2.7 Analysis

All spectral variables determined for adaxial and abaxial leaf surfaces were examined for N treatment responses, associations with leaf chemistry, and for correlations between optical and fluorescence parameters. The spectral variables included: original and derivative indices from the four types of optical spectra (RT, RB, TrT, and AT); the emissions extracted from fluorescence peaks in the blue, green, red and far-red spectral regions produced from 280EX and 380EX, and their ratios; the emissions at 685 and 740 nm produced from 532EX, and their ratio; and the FIS images produced in the blue, green, red, and far-red bands, and their ratios. The data sets were analyzed with a statistical package, Systat V8 and V9 (SPSS Inc., Chicago IL, USA) using the general linear model and analysis of variances (GLM, ANOVA). The significance of the differences among means was determined with the Tukey-Kramer test.

## 3. RESULTS

### 3.1 Descriptive data

Examples of the various optical and fluorescence data types acquired in this experiment are given in Figures 1-4. Average adaxial and abaxial emission spectra (280EX, 380EX, and 532EX) of corn leaves from the four N treatment groups acquired in September with the FluorologII spectrofluorometer are shown in Figure 1 (A,B,C). The Red/FR ratios (685F/740F) per N treatment resulting from 380EX and 532EX for abaxial surfaces of leaves determined in September are shown in Fig. 1D. The Red/FR ratios increased as N availability declined, and this was most expressed by the Red/FR<sub>EX532</sub> ratio ( $r^2 = 0.61$ ). Representative FIS images (Figure 2A) and FIS band averages for September per N treatment for both leaf surfaces are presented in Figure 2B and C. Different patterns across FIS bands are obvious for adaxial vs. abaxial surfaces: the fluorescence intensities were much higher for abaxial surfaces as compared to leaf tops; for adaxial surfaces the highest fluorescence was produced in the FR band and the lowest in the blue band (except for the 100% optimal group, or 140 kg N/ha). Whereas for the leaf undersides, both the red and FR bands associated with the ChlF peaks were consistently higher than the blue and green bands. The green band exhibited N treatment differences for abaxial surfaces, decreasing as more soil N was available (Fig. 2C).

The average derivative spectra for four optical properties [TrT, AT, RT, and RB] of adaxial and abaxial surfaces of corn leaves from the four N treatments, acquired on 9/17/01, are shown in Figure 3. The blue-ward shift of the first derivative maximum ( $D_{max}$ ) that occurs between 690 and 730 nm with reduced soil N availability is apparent. A subset of the data used to determine the fluorescence contribution to reflectance of one leaf surface is shown in Figure 4. Here, the decay from light-induced maximum ChlF ( $ChlF_{max}$ ) to steady state fluorescence ( $F_s$ ) for one leaf surface was determined from rapidly acquired repetitive scans.

The time trends for daily means per N treatment of several variables are shown in Figure 5. Chl *a* content (Fig. 5A) in August was similar in all leaves, but treatment differences were apparent in September when Chl *a* was higher (for 70, 140, 210 kg N/ha) or lower (28 kg N/ha) than in August. The Chl *a* content was apparently responding to rainfall received in the latter half of August. However, Chl *b* (Fig. 5B) was apparently more responsive to the light environment, and decreased relatively smoothly over time in August through September, with treatment differences achieved by the last date. A general decline in  $A_{max}$  was also observed, with treatment difference occurring early and late in the period examined (Fig. 5C). The foliar C/N ratio was similar and relatively low ( $< 12$ ) across N treatments in August but increased during September (Fig. 5D), most dramatically in the lowest N treatment. By the last date, statistically significant ( $P < 0.01$ ) increases in the foliar C/N ratio were observed. A similar trend over time was observed for the optical derivative index,  $D_{max}/D_{744}$  (Fig. 5E).

### 3.2 Regression Analyses

The red edge derivative ratio,  $D_{max}/D_{744}$ , was non-linearly associated with the C/N ratio (Figure 6) when determined from any of the four optical properties [23]. The coefficients of determination,  $r^2$  were: TrT = 0.86 (0.90 with N treatment groups included); AT = 0.82 (0.88); RT = 0.80 (0.85); and RB = 0.79 (0.85). About 5% more variance in  $D_{max}/D_{744}$  was explained by the C/N ratio when determined from TrT and AT spectra, as compared to RT and RB. Two fluorescence parameters were linearly related to the foliar C/N ratio (Figure 7), the Red/FR<sub>EX532</sub> ratio ( $r^2 = 0.75$ ) and the FIS green band ( $r^2 = 0.80$ ). The  $D_{max}/D_{744}$  red edge ratio was also non-linearly but inversely associated with the



Chl *b* content throughout the experiment for all four optical properties, shown for RT ( $r^2 = 0.91$ ) in Figure 8. Similar, but overlapping inverse quadratic relationships were obtained for the other three optical properties, for which  $r^2$  values were: AT = 0.90 (0.88 with N groups included); TrT = 0.89 (0.86); and RB 0.85 (0.81). The Red/FR<sub>EX532</sub> fluorescence ratio obtained from abaxial leaf surfaces was also related to Chl *b* content ( $r^2 = 0.76$ , Figure 8 inset frame). Consequently, both the optical red-edge ratio (Dmax/D744) and the ChlF ratio, Red/FR<sub>EX532</sub>, were related to two leaf constituents, the C/N ratio and Chl *b* content.

The C/N ratio was inversely dependent on Amax, with separate, linear curves per N group ( $r^2 = 0.85$ ; Figure 9A). The “X” axis approximates time, right to left, with greater foliar C/N content at the end of the season in all groups and higher C/N content in leaves grown in N deficient soils (e.g., 28 kg N/ha). Of twenty optical indices evaluated, only the 440/690 ratio determined from AT spectra [5, 19] was related to Amax ( $r^2 = 0.79$ ; Figure 9B). One fluorescence index, the Red/FR<sub>EX532</sub> ratio, was related to Amax ( $r^2 = 0.73$ ; Figure 9C).

For leaf abaxial surfaces, Dmax/D744 determined from any of the four optical properties was correlated with the Red/FR<sub>EX532</sub> ratio obtained from abaxial ChlF emissions (Figure 10). As before, the strongest associations were obtained for TrT and AT compared with RT and RB. The correlations (*r*) were: TrT = 0.95 (0.96, with N treatment groups included); AT = 0.94 (0.94); RT = 0.87 (0.90); and RB = 0.92 (0.95).

### 3.3 ChlF Contribution to Apparent Reflectance

The apparent reflectance (*R<sub>a</sub>*) measured in the Red and FR regions without the long pass filter was consistently higher than *R* measured with the filter. For the September leaves, 10-28% of *R<sub>a</sub>* at 685 nm and 3-6% of *R<sub>a</sub>* at 740 nm was due to ChlF. Values measured for *F<sub>max</sub>* and *F<sub>s</sub>* at the abaxial surface were always higher than for the adaxial surface at both ChlF peaks (685 and 740 nm; Table 1). *F<sub>max</sub>* represented 3-6% ( $\leq 15 \text{ W m}^{-2} \text{ sr}^{-1} \text{ } \mu\text{m}^{-1}$ ) of incoming radiation, whereas *F<sub>s</sub>* represented <2% ( $\leq 5.3 \text{ W m}^{-2} \text{ sr}^{-1} \text{ } \mu\text{m}^{-1}$ ) of incoming radiation in either ChlF peak (Tab. 1). The highest ChlF contribution to *R<sub>a</sub>* was observed for *F<sub>685max</sub>* (30-60 % of *R<sub>a</sub>*); however, the highest absolute ChlF occurred for *F<sub>740max</sub>* (3-14  $\text{W m}^{-2} \text{ sr}^{-1} \text{ } \mu\text{m}^{-1}$ ; Tab. 1). Although vegetation has relatively low *R* in the red edge region due to strong Chl *a* absorption, the relative contribution from steady state ChlF (*F<sub>s</sub>*) to *R<sub>a</sub>* is significant.

N treatment significantly affected the relationship between ChlF and *R*. A decrease in *F<sub>max</sub>* associated with soil N availability was observed for both leaf surfaces (Tab. 1). Optimal separation of the N treatments was achieved for the leaf adaxial surface using *F<sub>685s</sub>*, while *F<sub>740max</sub>* provided higher discrimination of N groups for the abaxial surface. The strongest treatment differences were expressed by the abaxial surfaces for three parameters: *F<sub>740max</sub>*, *F<sub>740slope</sub>*, and *F<sub>685slope</sub>*. For the both leaf surfaces under N deficiency, the relative *F<sub>s</sub>* fraction increased in concert with the nutrient stress levels (Figure 11). The ability to distinguish among N treatments was clearly improved for the abaxial surfaces, as shown for the *F<sub>685slope</sub>* variable (Figure 12) in agreement with the other results.

TABLE 1. CHANGES IN FLUORESCENCE PARAMETERS IN ASSOCIATION TO NITROGEN TREATMENT\*

Fluorescence parameter	Nitrogen treatment level (N in % of optimum, Means and $r^2$ )									
	Leaf adaxial (top) surface					Leaf abaxial (bottom) surface				
	0	50	100	150	$r^2$	0	50	100	150	$r^2$
<b>1. Fluorescence amount at 685 and 740 nm expressed as % of the incoming radiation</b>										
F685max (% Incoming)	2.98ns	2.65ns	2.51ns	2.65ns	0.35	3.53a	3.76ab	3.98b	3.48a	0.64
F685s (% Incoming)	<b>1.07a<sup>1</sup></b>	<b>0.79b</b>	<b>0.41c</b>	<b>0.67b</b>	<b>0.74</b>	0.98ab	1.21ab	1.36b	1.09a	0.51
F685slope	-0.076a	-0.06ab	-0.05b	-0.05ba	0.69	<b>-0.19a</b>	<b>-0.12b</b>	<b>-0.06c</b>	<b>-0.06c</b>	<b>0.79</b>
F740max (%Incoming)	3.48a	4.08bc	3.91b	4.40c	0.61	<b>4.29a</b>	<b>5.15b</b>	<b>5.71c</b>	<b>4.71b</b>	<b>0.89</b>
F740s (%Incoming)	<b>1.02a</b>	<b>1.04a</b>	<b>0.78b</b>	<b>1.03a</b>	<b>0.62</b>	1.28a	1.30ab	1.61b	1.29ab	0.45
F740slope	-0.11 ns	-0.10 ns	-0.09 ns	-0.10ns	0.46	<b>-0.24a</b>	<b>-0.20b</b>	<b>-0.13c</b>	<b>-0.12c</b>	<b>0.83</b>
<b>2. Fluorescence amount at 685 and 740 nm expressed as % of radiation reflected of the vegetation (<i>R<sub>a</sub></i>)</b>										
F685max (% of <i>R<sub>a</sub></i> )	35.8	30.8	46.7	44.9		46.8	49.3	61.4	52.3	
F685s (% of <i>R<sub>a</sub></i> )	15.2	11.0	10.0	12.8		15.5	16.2	28.3	24.7	
F740max (% of <i>R<sub>a</sub></i> )	9.5	8.8	11.4	12.0		11.0	12.2	14.5	11.8	
F740s (% of <i>R<sub>a</sub></i> )	5.5	4.5	3.1	3.3		3.4	3.7	5.0	5.0	
<b>3. Fluorescence amount at 685 and 740 nm (<math>\text{W/m}^2/\text{sr}/\mu\text{m}</math>)</b>										
F685max ( $\text{W/m}^2/\text{sr}/\mu\text{m}$ )	5.1	4.3	5.5	5.3		7.4	8.1	8.7	7.0	
F685s ( $\text{W/m}^2/\text{sr}/\mu\text{m}$ )	2.0	1.4	1.3	1.5		2.4	2.5	3.4	3.2	
F740max ( $\text{W/m}^2/\text{sr}/\mu\text{m}$ )	9.6	8.7	10.5	11.6		11.9	13.1	14.7	12.0	
F740s ( $\text{W/m}^2/\text{sr}/\mu\text{m}$ )	5.3	4.3	2.9	3.2		3.7	3.9	5.0	4.0	

\* Means are compared within row per leaf surface, significant differences among treatments with different letters (ANOVA).

<sup>1</sup> The highlighted text indicates the F regions of highest N treatment discrimination.

#### 4. DISCUSSION AND CONCLUSIONS

This experiment addressed the integration of optical and actively induced fluorescence measurements of corn leaves grown under different N regimes, assessing their relative utility in detecting physiological status near the end of the growing season when physiological conditions were changing. The biophysical leaf-level data for Chl *a*, Chl *b*, and C/N content, as well as for Amax, show that a range of growth conditions were captured over a seven week interval in the late summer of 2001. The foliar C/N allocation in leaves as a function of Amax throughout this period was affected by the soil N availability (Fig. 9A). The strongest association between a spectral index and a leaf constituent was achieved with the optical red-edge derivative index, Dmax/D744, versus either the C/N ratio or Chl *b* content. The Dmax/D744 index was successful for all optical properties (TrT, AT, RT, and RB). The strongest relationship of Dmax/D744 index to C/N content was achieved with TrT ( $r^2 = 0.90$ ; Fig. 6), whereas the strongest relationship to Chl *b* content was achieved with RT ( $r^2 = 0.91$ ; Fig. 8A). The strength of the relationships based on transmittance demonstrates the gain in information from all leaf tissues, whereas the reflectances are largely due to epithelial tissues. This study highlights the important role of N in altering photosynthetic function, carbon storage, and spectral responses.

Significant N treatment differences were expressed in the fluorescence Red/FR<sub>EX532</sub> ratio from abaxial leaf surfaces. As with the optical Dmax/D744 index, these were associated with changes in the C/N ratio ( $r^2 = 0.75$ ; Fig. 7A) and Chl *b* content ( $r^2 = 0.76$ ; Fig. 8B) over the study period. The FIS green band was also related to the C/N ratio ( $r^2 = 80$ ; Fig. 7B). Additionally, the FIS band emission patterns clearly distinguished adaxial from abaxial surfaces (Fig. 2B,C), and the green band was useful for discrimination of N treatments.

Several optical and fluorescence parameters were clearly able to separate N treatment regime levels under study. Similar N treatment responses were observed in the red edge with the Dmax/D744 index, the Red/FR<sub>EX532</sub> fluorescence ratio, and the first derivative maximum (Dmax) calculated from the steady-state (Fs) spectra used to determine the ChlF contribution to Ra (Fig. 12). However, the strongest evidence and confirmation of the interaction between the optical and fluorescence data was shown with the measurements of percent ChlF contribution to Ra in the Red and FR spectrum. On average, 10-25% of Ra was due to the steady-state fluorescence (Fs) at the 685 nm ChlF peak, and 2-6% at the 740 nm peak. The relationship between ChlF and Ra was significantly affected by the N treatments applied to the cornfields. This finding suggests that the use of passive ChlF in monitoring the physiological status of vegetation, already well established by the active ChlF technology, is likely applicable under natural solar illumination.

Our results indicate that the red edge spectral region is strongly responsive to foliar C/N content. Chl *a* was not as reliable a factor in affecting the red edge region, although Chl *b* was. The stronger responses were obtained for the abaxial surfaces may be useful to identify canopies experiencing environmental stress that causes changes in leaf display (e.g., adaxial → abaxial). These results demonstrate the potential of high spectral resolution data for remote determination of foliar C/N content, using derivative parameters such as Dmax/D744, Red/FR<sub>EX532</sub> ratio, and the green fluorescence emissions. These findings also increase our understanding of the dynamics of the red edge in relation to leaf photochemistry. Some aspects of this study were presently previously [22, 23].

#### ACKNOWLEDGMENTS

We wish to acknowledge Dr. Craig S.T. Daughtry and Dr. Timothy J. Gish (Hydrology and Remote Sensing Laboratory, USDA, Beltsville MD, USA) for their coordination efforts in developing the large long-term field site and campaign entitled "Economic and Environmental Enhancement (OPE3)" of which the current study was a part. The research was conducted under the NASA Terrestrial Ecosystems Program and funded by grant NASA#622-9247.

#### REFERENCES

1. ACCP, *Accelerated Canopy Chemistry Program*, Final Report Presented to EOS-IWG, 19 October, 1994.
2. J.R. Miller, J.R. Freemantle, M.J. Belanger, C.D. Elvidge and M.G. Boyer, "Potential for determination of leaf chlorophyll content using AVIRIS", *Proceedings of the 1993 Airborne Visible/Infrared Imaging Spectrometer (AVIRIS) Workshop*, JPL Pub. **72-77**, Pasadena, 1993.
3. M.E. Martin and J.D. Aber, "High spectral resolution remote sensing of forest canopy lignin, nitrogen, and ecosystem processes", *Ecological Applications*, **7**, pp. 431-443, 1997.



4. P.J. Zarco-Tejada, J.R. Miller., G.H. Mohammed, T.L. Noland and P.H. Sampson 1999, "Optical indices as bio-indicators of forest condition from hyperspectral CASI data", *Presented at the 19<sup>th</sup> symposium of the European Association of Remote Sensing Laboratories (EARSeL), Valladolid, Spain, 31 May – 2 June, 1999.*
5. Entcheva P. 2000. "Remote sensing of forest damage in the Czech Republic using hyperspectral methods", *PhD. Dissertation*, UNH, USA, 2000.
6. G.H. Mohammed, W.D. Binder and S.L. Gillies, "Chlorophyll fluorescence: a review of its practical forestry applications and instrumentation", *Scand. J. For. Res.*, 10:383-410 (1995).
7. M. Kim, C. Mulchi, J. McMurtrey C. Daughtry, and E. Chappelle, "Assessment of environmental plant stresses using multispectral steady-state fluorescence imagery", *Chapter 17, pp. 321-421, Air Pollution & Plant Biotechnology*, K.Omasa, H. Saji, S. Youssefian, N. Kondo (Eds.). ISBN 4-431-70216-4 Springer-Verlag, Tokyo, 2002.
8. H. K. Lictenthaler and U. Rinderle, "Role of chlorophyll fluorescence in the detection of stress conditions of plants", *CRC Critical Rev. Anal. Chem.*, **19**, pp. 29-85, 1988.
9. Chappelle, E., Wood, F., McMurtrey, J., & Newcomb, W. (1984), Laser induced fluorescence (LIF) of green plants, *Applied Optics*, 23:134-142.
10. L. Corp, J. McMurtrey, E.Chappelle, M. Kim and C. S. T. Daughtry, "Optimizing fluorescence excitation wavelengths for the detection of stress in vegetation", *Proc. Internat. Geoscience and Remote Sens. Symp.* **3**, pp. 1812-1815, 1996.
11. E. Middleton, E. Chappelle, T. Cannon, P. Adamse and S. Britz, "Initial assessment of physiological response to UV-B irradiation using fluorescence measurements", *J. Plant Physiol.*, **148**, pp. 68-77, 1996.
12. J.E. McMurtrey, E.W. Chappelle, M.S. Kim, J.J. Meisinger, and L. Corp, "Distinguishing nitrogen fertilization levels in field corn (*Zea mays* L.) with actively induced fluorescence and passive reflectance measurements", *Remote Sens. Environ.*, **47**, pp. 36-44, 1994.
13. E.W.Chappelle, M.S. Kim, and J.E. McMurtrey, "Ratio analysis of reflectance spectra (RARS): An algorithm for the remote estimation of the concentrations of chlorophyll *a*, chlorophyll *b*, and carotenoids", *Remote Sens. Environ.*, **37**, pp.121-128, 1992.
14. L. A. Corp, J. E. McMurtrey, E.W. Chappelle, M.S. Kim, "Physical properties of leaf level fluorescence", *Advances in Laser Remote Sensing for Terrestrial and Oceanographic Applications*, SPIE's AeroSense '97 **3059**, pp. 32-40, 1997.
15. M.S. Kim, J.E. McMurtrey, C.L. Mulchi, C.S.T. Daughtry, G. Deitzer and E.W. Chappelle, "Steady-state multispectral fluorescence imaging system for plant leaves", *Applied Optics*, **40**, pp. 157-166, 2001.
16. G. A. Carter, "Ratios of leaf reflectances in narrow wavebands as indicators of plant stress", *International Journal of Remote Sensing*, **15**, pp. 697-703, 1994.
17. G. A. Carter and A. K. Knapp, "Leaf optical properties in higher plants: linking spectral characteristics with plant stress and chlorophyll", *American Journal of Botany*, 2002, in press.
18. J.A. Gamon, L. Serrano and J.S. Surfus, " The photochemical reflectance index: an optical indicator of photosynthetic radiation use efficiency across species, functional types, and nutrient levels", *Oecologia*, **112**: pp. 492-501, 1997.
19. P. Zarco-Tejada, "Hyperspectral remote sensing of closed forest canopies: estimation of chlorophyll fluorescence and pigment content", *PhD. Dissertation*, 210 pp, York University, Toronto, Ontario, Canada 2000.
20. J.E. Vogelmann, B.N. Rock and D.M. Moss, "Red edge spectral measurements in sugar maple leaves", *Int. Journ. Remote Sens.*, **14**, pp. 1563-1575, 1993.
21. M.S. Kim, E.W. Chappelle, L.A. Corp, and J.E. McMurtrey, "The Contribution of chlorophyll fluorescence to the reflectance spectra of green vegetation", *Proc. Internat. Geoscience and Remote Sensing Symposium*, IGARSS '93 Digest, **3**, pp. 1325-1328, 1993.
22. P.K. Entcheva Campbell, E. M. Middleton, L.A. Corp, J.E. McMurtrey III, M.S. Kim, E.W. Chappelle, and L. M. Butcher, "Chlorophyll fluorescence and apparent red/near-infrared reflectance of corn foliage subjected to nitrogen deficiency", *Proceedings, 2002 IEEE International Geophysicscience and Remote Sensing Symposium (IGARSS2002)*, Toronto, Canada, June 23-27, 2002.
23. E.M. Middleton, P. K. Entcheva Campbell, J.E. McMurtrey, L.A. Corp, L. M. Butcher, and E.W. Chappelle, "Red Edge optical properties of corn leaves from different nitrogen regimes", *Proceedings, 2002 IEEE International Geophysicscience and Remote Sensing Symposium (IGARSS2002)*, Toronto, Canada, June 23-27, 2002.

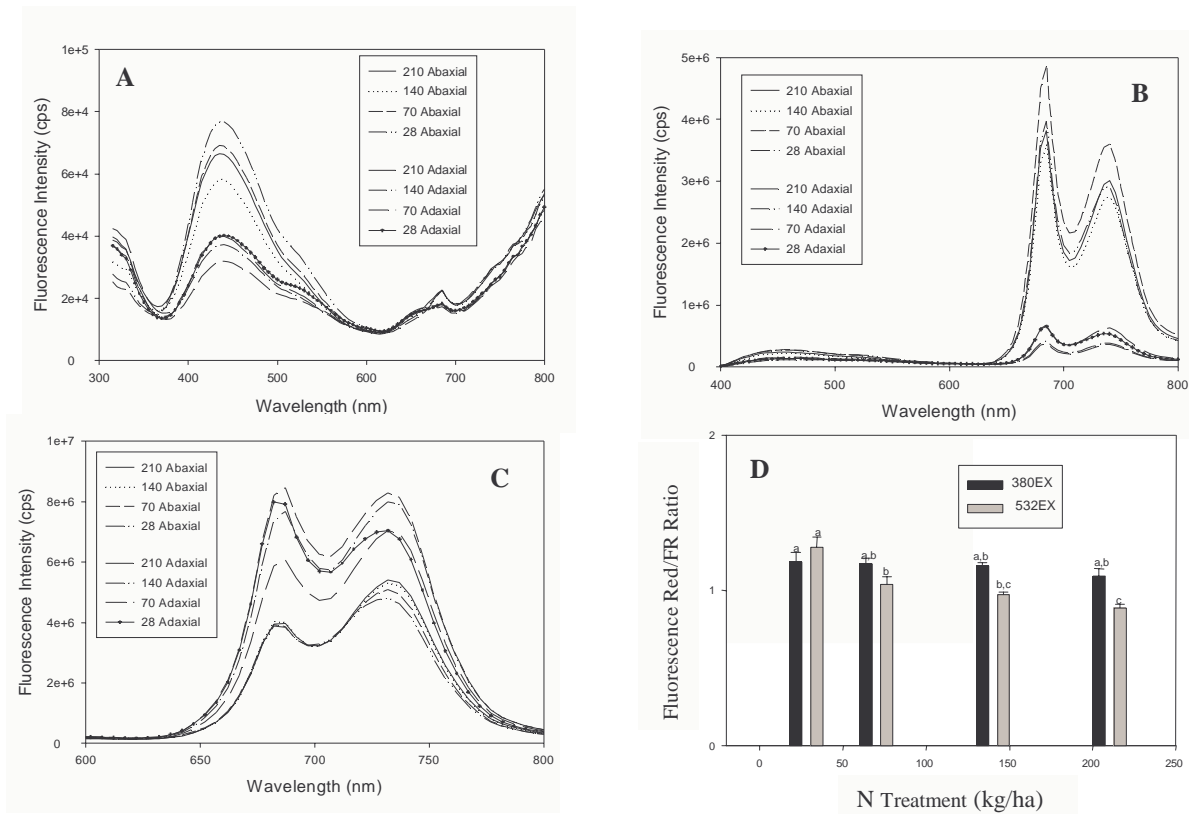


**Figure 1.** The September group averages (5 dates) for fluorescence emissions of upper canopy corn leaves from the four N treatments (28, 70, 140, 240 kg N/ha) acquired with the Fluorolog II spectrofluorometer are shown: **A)** emission spectra of abaxial and adaxial surfaces, produced from 280EX; **B)** emission spectra of abaxial and adaxial surfaces, produced from 380EX; **C)** emission spectra of abaxial and adaxial surfaces, produced from 532EX; and **D)** the means ( $\pm$  SE) for the Red/FR ratio for chlorophyll emissions resulting from 380EX (Red/FR<sub>EX380</sub>) and 532EX (Red/FR<sub>EX532</sub>) of abaxial surfaces. An increase in the ratio as soil N level decreased is significant for both ratios, especially when the time trends over two weeks are included, but the results for the Red/FR<sub>EX532</sub> ratio are much stronger ( $r^2 = 0.61$ ,  $P = 0.001$ ) than for R/FR<sub>EX380</sub> ( $r^2 = 0.36$ ,  $P = 0.02$ ). The GLM model included N treatment and date as grouping factors.

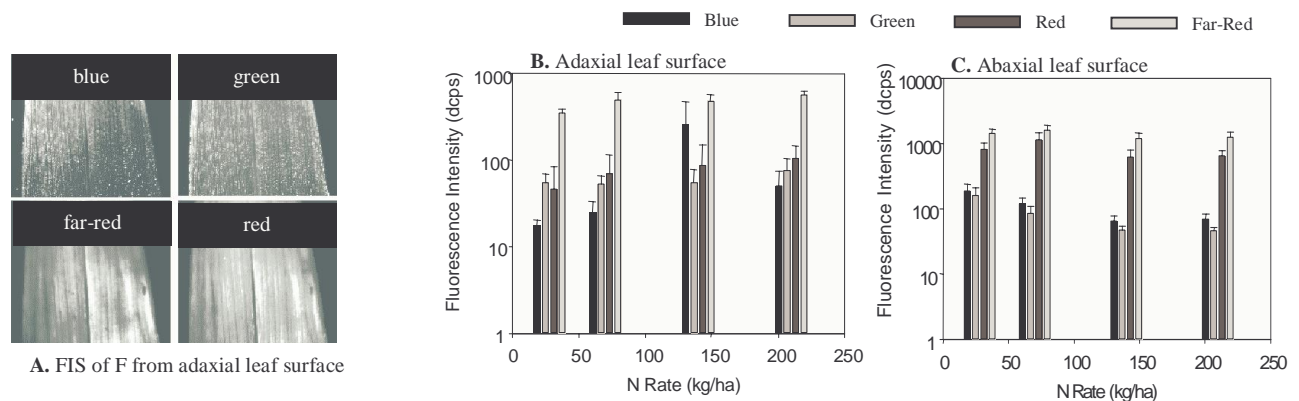


**Figure 2.** FIS data acquired for upper canopy corn leaves in September are shown: **A)** the four band (blue, green, red, and far-red) FIS images of adaxial surfaces acquired on 9/17/01; and **B)** the FIS band fluorescence intensities (dcps) for adaxial surfaces of leaves from the four N treatments, mean ( $\pm$  SE) for 5 dates in September; and **C)** the corresponding FIS band fluorescence intensities (dcps) for abaxial surfaces of leaves per N treatment, mean ( $\pm$  SE) for 5 dates in September. The Y axis scale for abaxial fluorescences (C) is an order of magnitude greater than adaxial values (B). The green fluorescence of abaxial surface (C) decreased significantly as N rate (kg/ha) increased: 28(a), 70(ab), 140(c), and 240(c).

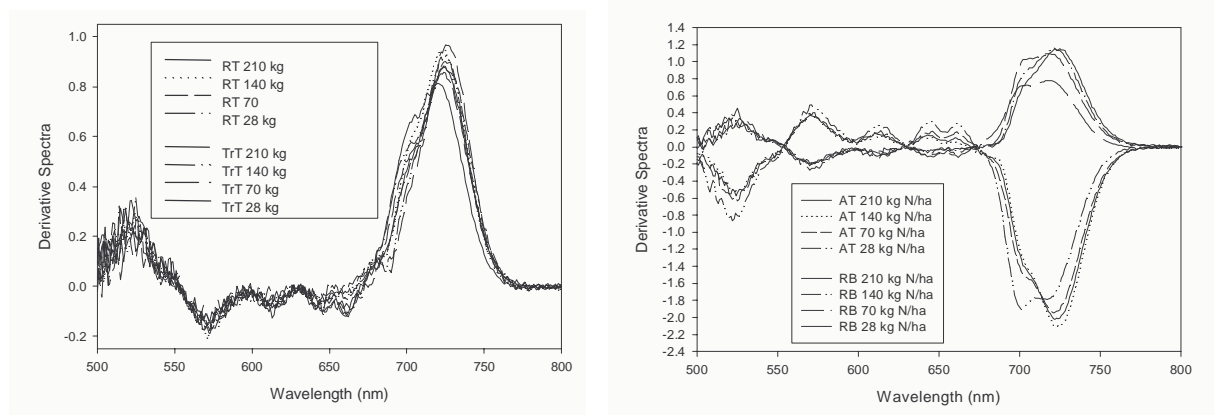


**Figure 3.** The first derivative spectra (500 - 800 nm) for four optical properties [RT, TrT, RB, and AT] of upper canopy corn leaves from the four N treatments, acquired on 9/17/01: **A)** RT and TrT adaxial spectra; and **B)** RB abaxial spectra and AT adaxial spectra.

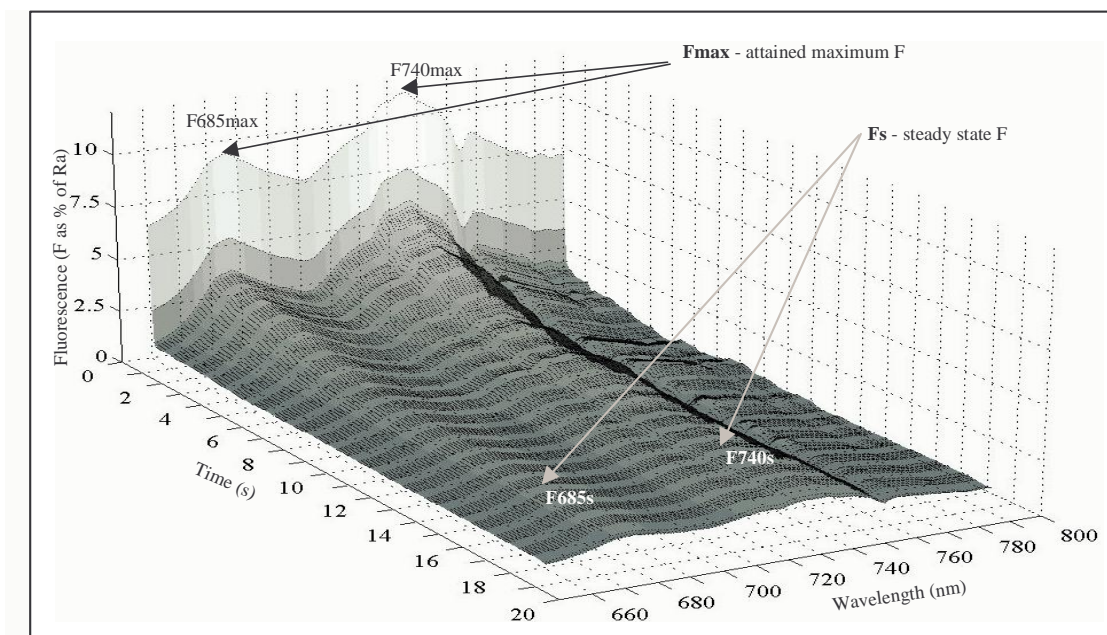


**Figure 4.** Foliar fluorescence emissions (example for abaxial surface) obtained using the optical instrumentation setup to determine the contribution of ChlF to “apparent reflectance” ( $R_a$ ) in the red and far-red spectrum is shown. This data set measures  $R_a (= R + \text{ChlF})_\lambda$  and is acquired at 0.01 s over 25 s *without* the RG 665 Schott filter placed in front of the light. This data set is paired with a similar set of spectra acquired *with* the filter to measure  $R$  (true reflectance). The ChlF contribution to  $R_a$  is determined from the difference of these two datasets. Here,  $R_a$  of the dark-adapted leaf exhibits the classic characteristics of ChlF induction kinetics: immediate expression of ChlFmax, followed by decay to the steady state ChlF within ~20 s.

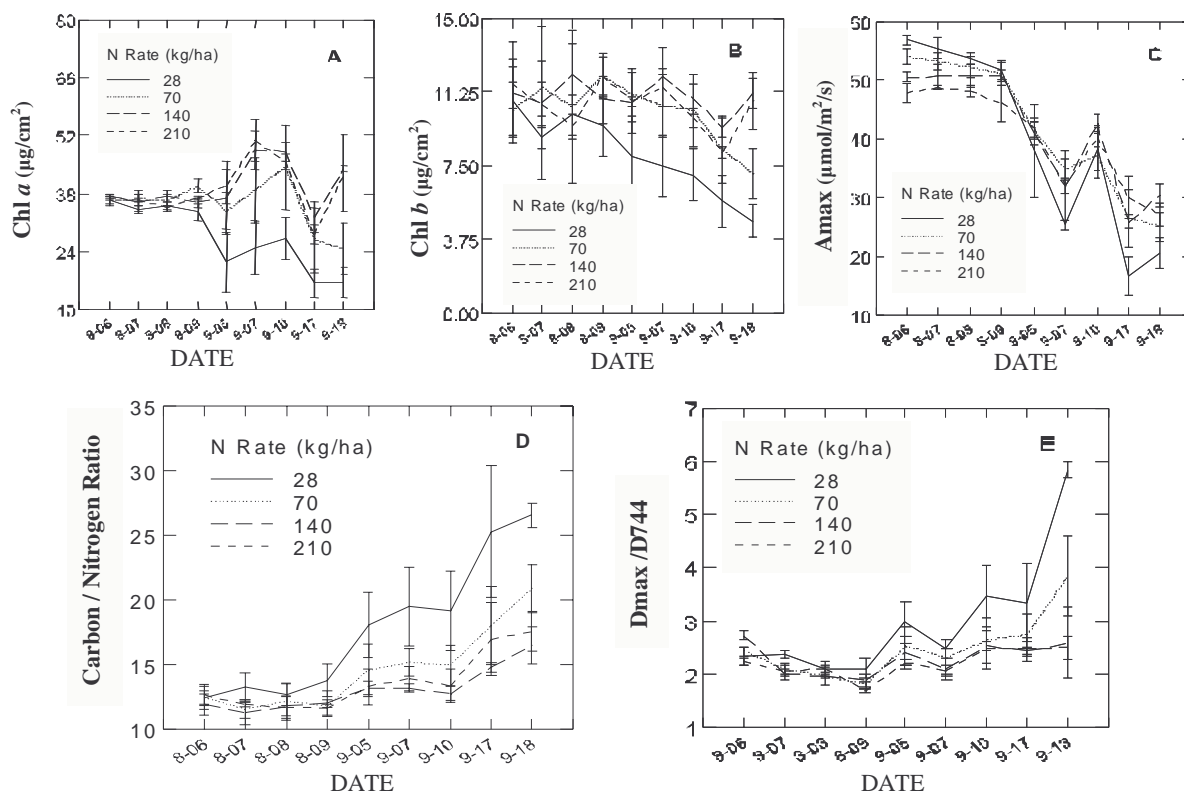


**Figure 5.** The daily means of several leaf parameters for upper canopy corn leaves from four field plots with different nitrogen fertilizer applications (28, 70, 140 and 240 kg N/ha). Daily means per group ( $\pm$  SE) were acquired on nine days in August and September 2001. Variables presented are: **A)** Chl *a* ( $\mu\text{g cm}^{-2}$ ); **B)** Chl *b* ( $\mu\text{g cm}^{-2}$ ); **C)** Amax, photosynthetic capacity ( $\mu\text{mol CO}_2 \text{ m}^{-2} \text{ s}^{-1}$ ); **D)** foliar C/N ratio (% dry mass); and **E)** the red-edge derivative ratio, Dmax/D744.

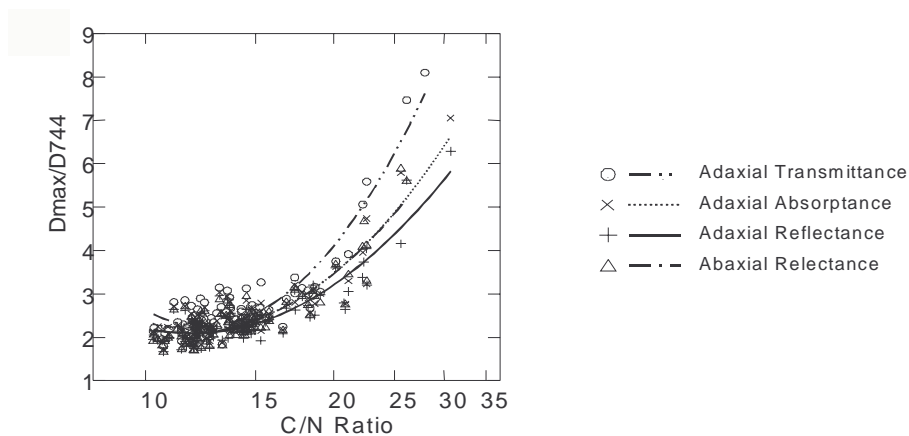


**Figure 6.** The red edge derivative ratio, Dmax/D744, as a function of foliar C/N content (% dry mass) is shown for upper canopy corn leaves. Separate curves are given for each of the four optical properties: adaxial transmittance (TrT); adaxial absorbance (AT); adaxial reflectance (RT); and abaxial reflectance (RB). The relationship of Dmax/D744 ratio to the log of C/N content is non-linear (quadratic):  $r^2$  values for the TrT, AT, RT, and RB curves are 0.86, 0.82, 0.80 and 0.79, respectively. The N treatment groups accounted for 4-6% additional variation, producing  $r^2$  values of 0.90, 0.88, 0.85, and 0.85 for TrT, AT, RT, and RB, respectively (not shown).

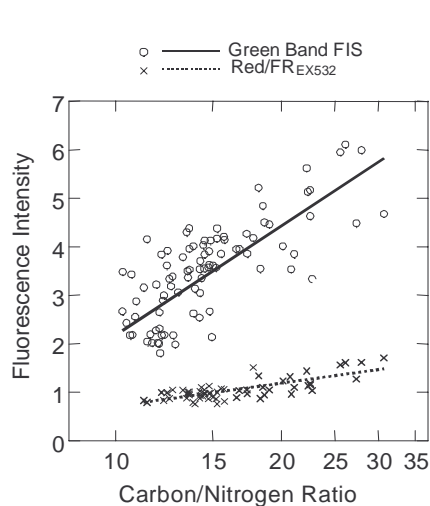


**Figure 7.** The log-log linear relationships of two fluorescence parameters to the foliar C/N ratio for upper canopy corn leaves: lower curve, the Red/FR<sub>EX532</sub> ratio,  $r^2 = 0.75$ ; upper curve, the FIS green band,  $r^2 = 0.80$ .

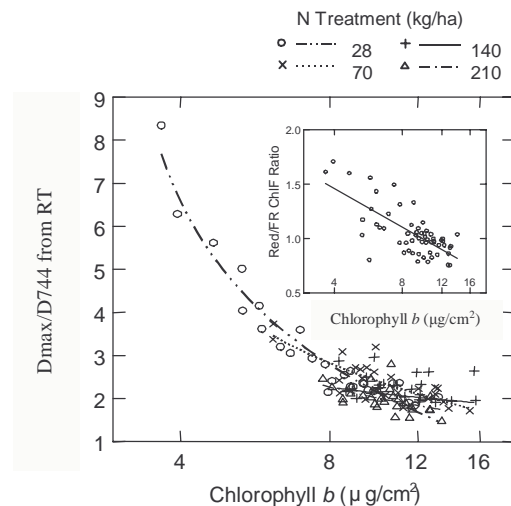


**Figure 8.** The relationships of two spectral indices as a function of the foliar Chl *b* content ( $\mu\text{g cm}^{-2}$ ) for upper canopy corn leaves are given. The large frame shows the red edge derivative ratio (Dmax/D744) determined from RT spectra, as an inverse non-linear relationship to the log (Chl *b* content). When N treatment groups are included in the model, as shown with separate curves, the  $r^2 = 0.91$ ; without inclusion of the N groups, the  $r^2 = 0.88$ . The smaller, inset frame shows the Red/FR<sub>EX532</sub> fluorescence ratio determined from the abaxial surfaces, as an inverse linear relationship to the log (Chl *b* content),  $r^2 = 0.76$ .

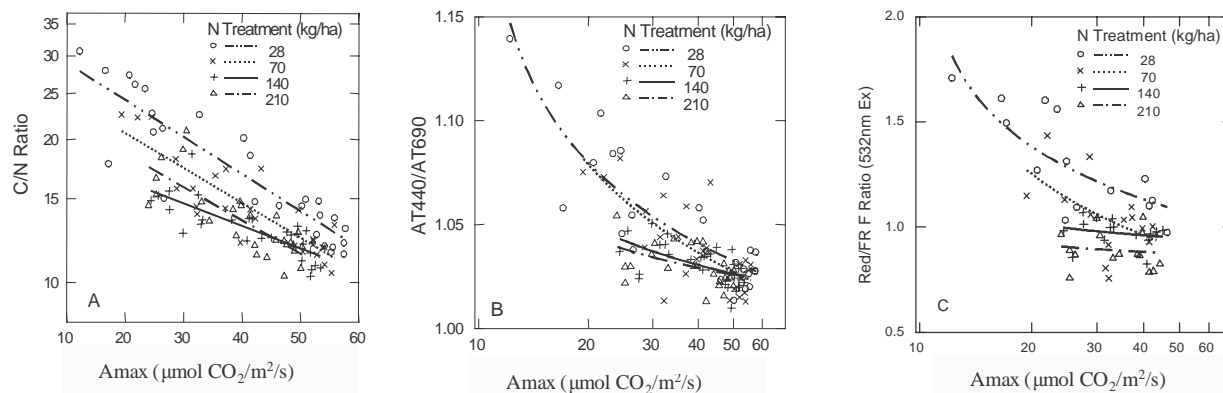


**Figure 9.** The inverse relationships of three variables to Amax are given for upper canopy corn leaves, with separate curves for the four N treatments: **A)** the foliar C/N ratio,  $r^2 = 0.85$  (over all treatments); **B)** an optical spectral index calculated from AT spectra,  $r^2 = 0.79$  (over all treatments), AT440/AT690 (absorptances: 440 nm / 690 nm; and **C)** the Red/FR<sub>EX532</sub> fluorescence ratio,  $r^2 = 0.73$  (over all treatments).



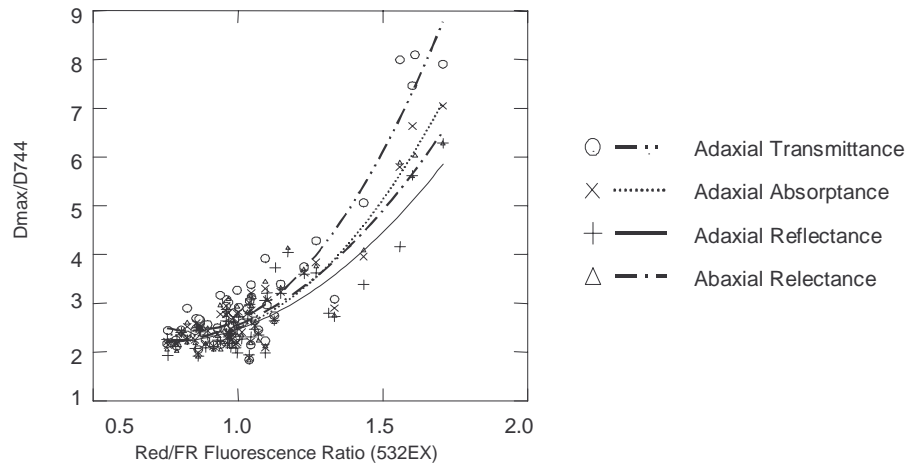


**Figure 10.** The correlation between the rededge derivative ratio,  $D_{\max}/D_{744}$ , to the  $\text{Red}/\text{FR}_{\text{EX532}}$  fluorescence ratio determined from the abaxial surfaces (undersides) of upper canopy corn leaves: **A)** Separate curves are given for each of the four optical properties (AT, TrT, RT and RB) yielding these correlations ( $r$ ): TrT = 0.95 (0.96, including the N groups), AT = 0.94 (0.94), RT = 0.87 (0.90), and RB = 0.92 (0.95). Including the N treatment group as a factor produced slightly higher (~1-3%) correlations

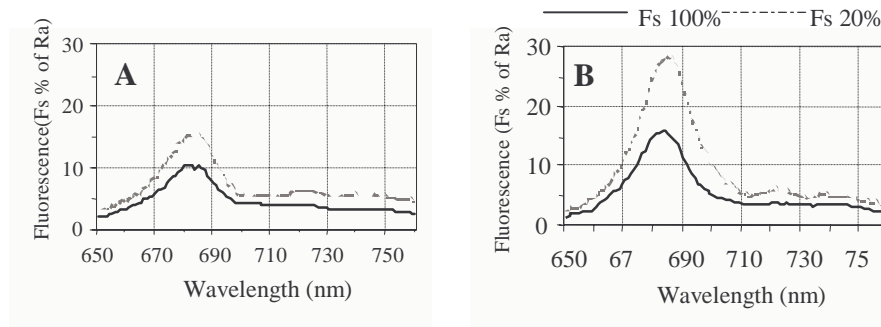


**Figure 11.** The relative contributions of steady-state ChlF at 685 nm to “apparent reflectance” (Ra) for the 20% and 100% N treatment groups (28 and 140 kg N/ha) are shown: **A)** adaxial surface and **B)** abaxial surface.

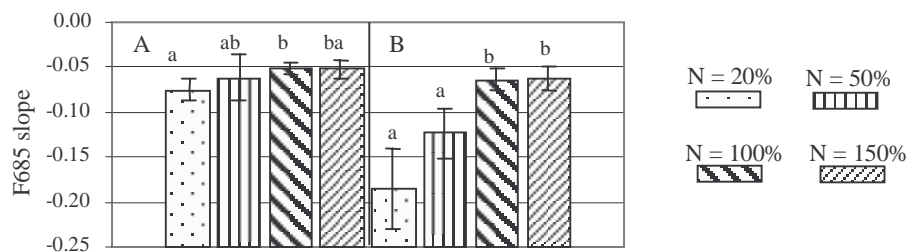


**Figure 12.** The means ( $\pm$  SE) of the September dates for F685slope (the first derivative of the time spectra of 685 nm measurements) which expresses the rate of change as F685max decays to F685s over time ( $< 30$  s), for the four N treatments: **A)** adaxial surface ( $r^2 = 0.45$ ); and **B)** abaxial surface ( $r^2 = 0.83$ ).